Geophysical Journal International

Geophys. J. Int. (2010) doi: 10.1111/j.1365-246X.2010.04759.x

Magmatic underplating of crust beneath the Laccadive Island, NW Indian Ocean

Sandeep Gupta, Santosh Mishra* and S. S. Rai

National Geophysical Research Institute (CSIR), Hyderabad-500 007, India. E-mail: sandeep.ngri@gmail.com

Accepted 2010 August 3. Received 2010 July 20; in original form 2010 March 17

SUMMARY

We investigate the crust and uppermost mantle velocity structure beneath the Laccadive Island through the inversion of teleseismic receiver functions following the neighbourhood algorithm. The velocity structure suggests that the 16-km thick-oceanic crust is underplated by 8-km thick high-velocity layer ($Vs \sim 4.25$–4.4 km s^{-1}; $Vp \sim 7.35$–7.6 km s^{-1}). The uppermost mantle shear velocity is ∼4.6 km s^{-1} ($Vp \sim 8.18$ km s^{-1}). The Moho at 24 km is possibly formed due to underplating of mantle-derived picritic melt at the base of oceanic crust produced during the interaction of the Indian plate with the Reunion hotspot. Continuity of crustal-underplated material beneath the Laccadive could be traced to the Laxmi Ridge in the north and to the Reunion Island in the south, suggesting this to be possible trace of the Reunion hotspot.

Key words: Composition of the oceanic crust; Dynamics: seismotectonics; Hotspots; Crustal structure; Indian Ocean.

1 INTRODUCTION

The Laccadive Island is a part of the Chagos–Laccadive Ridge (CLR), a prominent aseismic topographic/tectonic feature of the southwest continental margin of India (Fig. 1) extending 75–100 km in east–west direction (72°–74°E) between 7°N and 15°N. Further in south, it could be traced to 10°S in an arcuate fashion (Schlich 1982). Based on deep-sea drilling data the average age of the CLR (between 3°N and 10°N) is inferred to be 60 Ma (Fisk *et al.* 1989). The CLR has conspicuous higher gravity values than the basins on either side (Naini & Talwani 1982) in a regional negative free air anomaly. It is widely hypothesized to be the trace of the Reunion hotspot (Wilson 1963; Morgan 1972; White & McKenzie 1989). Despite its significance in providing critical linkage between the hotspot and genesis of islands, the Laccadive Island is poorly investigated using modern seismological tools and the basic information related to the Moho depth and nature of intracrustal layering is incomplete.

The early seismic study (Francis & Shor 1966) on unreversed line, near the Maldive Island (Fig. 1) suggests oceanic sequence with layers much thicker than usual with overlying water depth ∼2–2.5 km and the Moho at 16–20 km depth. We present here seismic velocity structure beneath the Laccadive Island segment of the coral-capped Chagos–Laccadive Island Ridge through modelling of teleseismic receiver functions (RF).

2 DATA

We used data from two temporary broad-band seismic stations, placed approximately 200 m apart, at Minicoy (the Laccadive Island) during 2005 January–April (Fig. 1). The stations configurations include CMG-3T sensors with a flat velocity response between 0.008–50 Hz and REFTEK 130–01 data loggers. Data were continuously recorded at 20 samples and GPS time logged.

Considering noise condition on the island, to enhance signal-to-noise ratio (S/N), we stacked the waveforms from both the stations (and named LAK); and to minimise the influence of the sea noise on the RF, a two-pole high pass filter with a corner frequency of 0.05 Hz was applied to the stacked teleseismic events. We computed RF using iterative time domain deconvolution approach (Ligorria & Ammon 1999) from 72 earthquakes of good S/N ratio and magnitude >5.5 in the epicentral distance range 30°–95° (Fig. 2). RF was calculated using Gaussian pulse width corresponding to low pass filter with corner frequency of 2.4, 1.25, 0.7 and 0.5 Hz. For further analysis we used only the RF with variance reduction cut-off above 80 per cent and the direct *P* within 1 s of the zero time on the deconvolved trace. At higher frequencies, RF was noisy whereas at lower frequency they smooth out. This in view to map the crust–mantle boundary along with other intracrustal layers, we preferred to use the RF with Gaussian width 1.6 for further analysis and modelling (Fig. 3). Due to the shorter duration of the experiment we could get fewer usable RF from different directions.

The RFs show shift in direct *P* arrival by ∼0.7 s, suggestive of thin near surface low velocity layer. Other observed phases (converted and multiples) are at ∼3.45, 6.95, 10.25 s (positive polarity) and at 5.25, 8.50, 12.10 s (negative polarity). First visible positive amplitude (backazimuth >65°) at ∼3.45 s with well-defined multiples at ∼10.25 and ∼12.10 s; corresponds to depth of 25–28 km. The absence of this phase for the northeastern backazimuth events (∼8°–55°) could be due to interference of conversions with multiples from of middle crustal discontinuities. Other consistent positive polarity (at ∼6.95 s) with negative polarity (∼8.50 s) could

*Now at: GeoSolutions (OBP), WesternGeco, Schlumberger, United Kingdom.

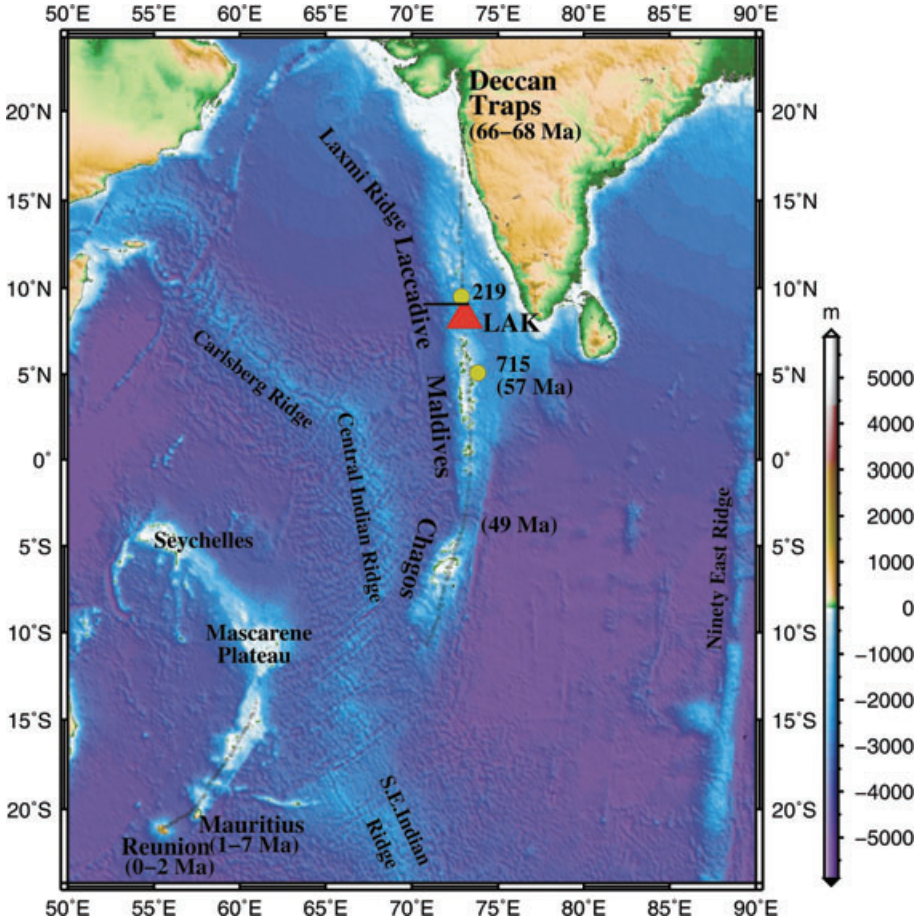

Figure 1. Tectonic map of western and central Indian Ocean, showing location of broad-band seismic station (red triangle), trail of the volcanic ridges and islands (Reunion, Chagos–Maldive–Laccadive and Laxmi) left by the Reunion plume as India migrated northward (dotted line). Also shown are refraction profile by Francis & Shor (1966) (solid line), DSDP sites (filled circle) and average age of the rocks in Ma (in parentheses). (Modified from White & McKenzie 1989).

be multiples of conversion at ∼1.7 s (merged within other phase) and corresponds to depth range of ∼13–17 km.

3 RF MODELLING

To minimize the effects of noise and aid in visually enhancing coherent arrival, radial RFs with good S/N ratio were stacked in a ±4° epicentral distance and backazimuth bins. Fig. 4 shows the six individual RFs for backazimuth 102° and epicentre distance 55°. The stacked RF (with bounds) shown at the bottom of Fig. 4 was used to determine the velocity structure beneath the seismograph location.

We mapped the *S*-wave velocity (*Vs*) with depth beneath the Laccadive Island from the observed stacked radial RF following the non-linear neighbourhood algorithm proposed by Sambridge (1999, 2001). The method assumes 1-D isotropic velocity model. It is a multidimensional parameter space search algorithm that only needs solving the forward problem and does not require computing partial derivatives of the RF. This method uses an ensemble-based Monte Carlo search technique to find the set of velocity models, which best satisfy the objective function. We used, as our objective function, a scaled L2-norm of the difference between the theoretical and the observed RF.

In this study, we used a time-window of 18 s and a 24-D parameter space, defined by six flat layers each with four parameters (layer thickness, *S*-wave velocity at the top and bottom of each layer and *Vp/Vs* ratio). The two *S*-wave velocity parameters in each layer allow definition of a velocity gradient for that layer, which allows representation of a large number of potential velocity-depth distributions. Very loose *a priori* constraints were placed on the minimum and maximum *S*-wave velocities, the layer thicknesses, as well as *Vp/Vs*. The model parameterization is shown in Table 1. Each inversion run involved 200 iterations, generating 20100 velocity models. Stability of the inversion solutions was tested using a large range of initial random seeds, incidence angles and velocity model parameters. The calculated RF (dashed line) and the observed stacked RF (solid line) are shown in Fig. 5(a). In Fig. 5(b), the best fit *S*-wave velocity model (solid red line) along with all other models (solid grey lines) that fit the RF are also displayed. The green region depicts best 1000 velocity models and blue line shows the *Vp/Vs* ratio variation for the best model (Fig. 5b). The 1-D velocity model obtained by the inversion process is able to model the dominant phases in the RF. Geographical location of study area places restrictions on the azimuthal distribution of recorded earthquakes. In a short duration experiment, therefore it was not possible to investigate anisotropy or effect of dip using RF modelling.

4 RESULTS

The RF study presented here provides *S*-wave velocity (*Vs*) variation with depth, whereas the earlier published results in the

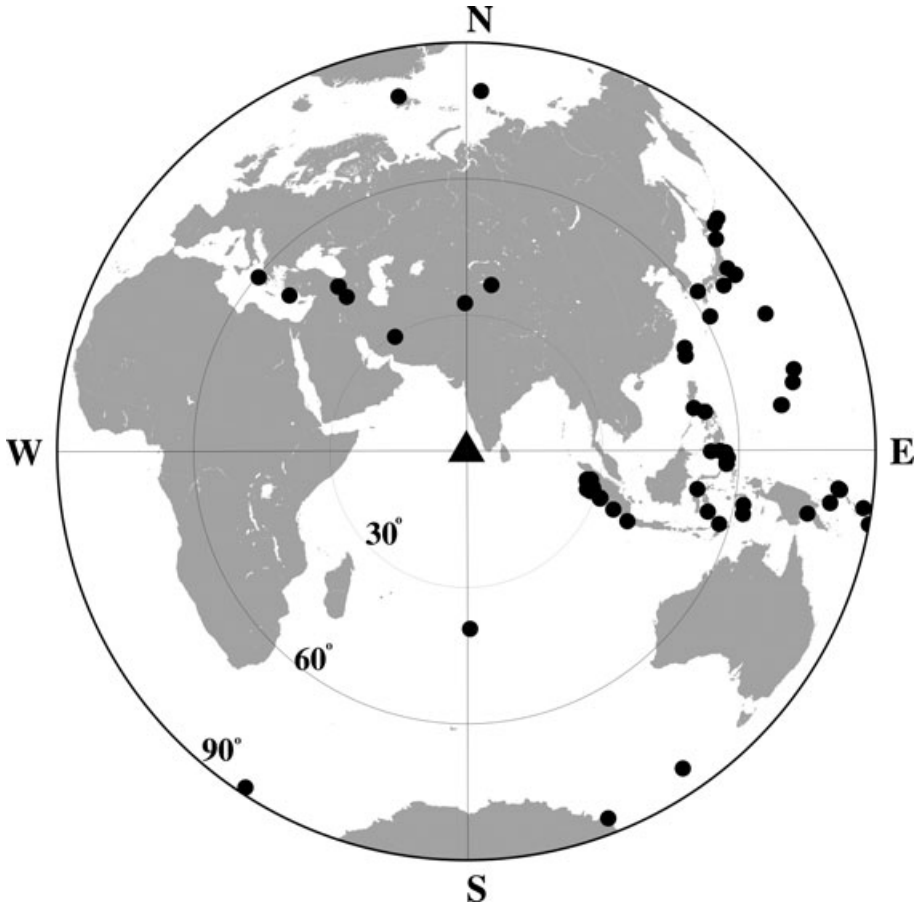

Figure 2. Epicentral locations of the teleseismic events (dots) used in this study. The triangles denotes the seismic station.

neighbourhood of the study area have only *P*-wave velocity variation with depth. To ensure comparisons, we also provide *P*-wave velocity (*Vp*), along with *S*-wave velocity (*Vs*), using the inferred *Vp/Vs* ratio of the individual layer. We discuss below the details of the velocity model (Fig. 5b) in the context of an oceanic environment (Christensen & Salisbury 1975). Layer 1: ∼1.5 km thick layer of velocity $Vs = 1.3$–2.8 km s^{-1} ($Vp/Vs = 1.9$–1.82; $Vp = 2.5$–5.0 km s^{-1}) is near surface low velocity possibly representing the soft sediments and coral (Francis & Shor 1966). Layer 2: Between 1.5 and 7.0 km a layer with velocity $Vs \sim 3.0$–3.3 km s^{-1} ($Vp/Vs = 1.79$–1.77; $Vp = 5.4$–5.8 km s^{-1}) is mapped that can be interpreted as the oceanic basement (Pichon *et al.* 1965). This is also in agreement with drilling results on the DSDP site 219 (9.03°N, 72.88°E, Fig. 1), showing presence of volcanic rock at about 1.5 km depth (Whitmarsh *et al.* 1974). Layer 3: Below the oceanic basement, between 7 and 16 km, we infer ∼9 km thick layer with typical oceanic lower crustal velocity ($Vs = 3.6$–4.1 km s^{-1}; $Vp/Vs = 1.76$–1.71; $Vp = 6.4$–7.0 km s^{-1}). Further down, between 16 and 24 km, we modelled ∼8 km thick layer of $Vs = 4.25$–4.4 km s^{-1} ($Vp/Vs = 1.74$–1.72; $Vp = 7.35$–7.65 km s^{-1}) followed by another higher velocity layer ($Vs \sim 4.6$ km s^{-1}, $Vp/Vs = 1.76$, $Vp \sim 8.15$ km s^{-1}).

To asses the reliability of the preferred velocity model, in particular the presence of high velocity layer at depth 16–24 km, we carried out synthetic tests with varying velocities. Fig. 6(a) and (b) shows that the phases at ∼3.45 s and ∼6.95 s are well matched with the presence of high velocity lower crustal layer and the presented velocity model is reliable.

5 DISCUSSION

We interpret the velocity model in term of existing knowledge of the oceanic crust parameters and processes of its formation (White *et al.* 1992). The Moho is the first-order discontinuity between the lower crust of *P*-wave velocity ∼7.0 km s^{-1} and the upper-mantle of *P*-wave velocity >7.8 km s^{-1}. Beneath the Laccadive, top 16 km has *P*-wave velocity <7.0 km s^{-1} with the thickness of igneous part (layer 2 + layer 3) of the crust as ∼14.5 km. This is also corroborated by the rare earth element inversion of the geochemical samples off the CLR that suggests the melt thickness of 13.7 km (White *et al.* 1992).

An 8 km thick layer of *P*-wave velocity ∼7.35–7.65 km s^{-1} is modelled between 16 and 24 km. This is possibly representing the material intermediate between gabbro ($Vp = 6.7$–7.2 km s^{-1}) and peridotite ($Vp = 7.8$–8.3 km s^{-1}), suggesting rock composition between mafic and ultramafic. The detailed geochemical and petrological analysis of the basalt from the DSDP site 715 (57 Ma) in the northern Maldives (Fig. 1) suggests similarity between the lava from the site and the Reunion hotspot (Fisk *et al.* 1989). Further, petrological models of magma genesis beneath hotspot show that the mafic cumulus ($Vp = 7.5$–7.9 km s^{-1}) along with intrusions of gabbros ($Vp = 6.8$–7.0 km s^{-1}) in the upper crust can be obtained by the crystal fractionation of the picritic primary melts, formed at 20 and 30 kbar (Farnetani *et al.* 1996). In view of the above, we hypothesize that the 16 km boundary represents the oceanic crust followed by 8 km thick underplating leading to the altered 'Seismic Moho' at a depth of 24 km. Similar observations were

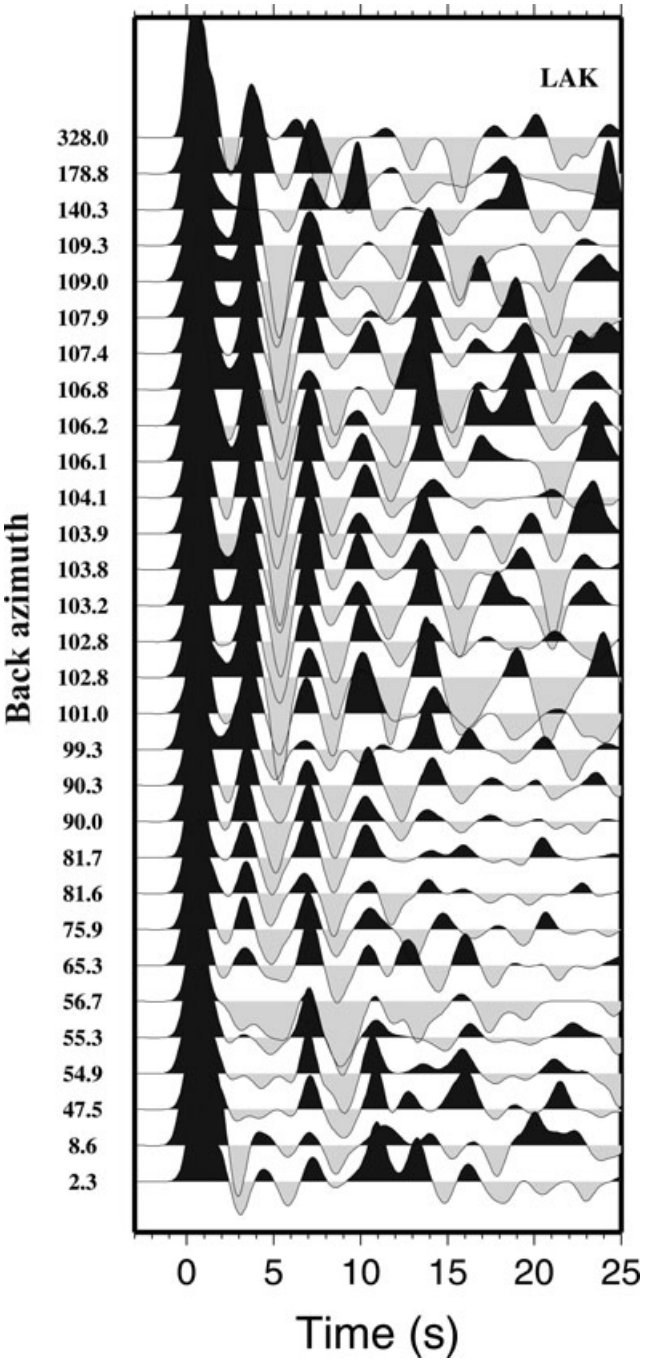

Figure 3. Equidistance plot of stacked radial receiver functions, plotted with reference to backazimuth.

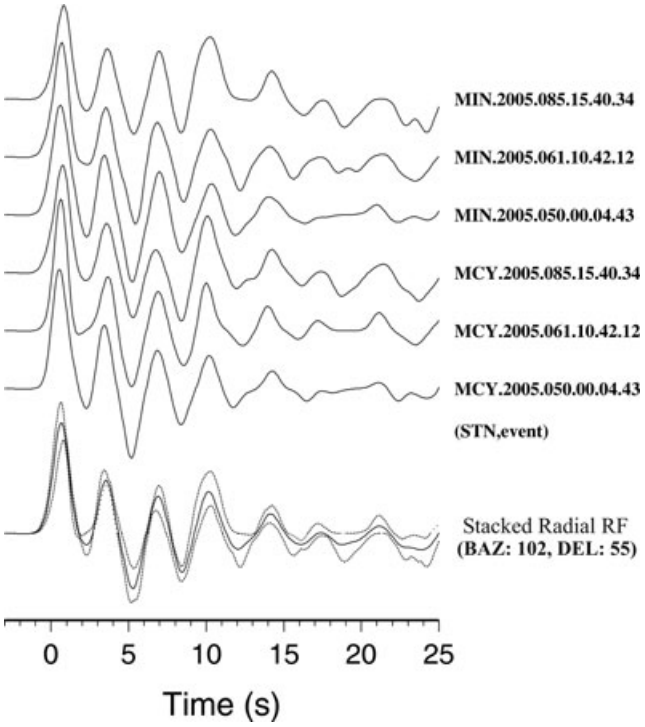

Figure 4. Plot of six individual radial receiver functions used to get stacked radial receiver function for modelling. The ±1 standard deviations are shown as dotted line.

Table 1. Parameter space bound used in the receiver function inversion. Brackets show indices.

Layer	H (km)	Vs_1 (km s^{-1})	Vs_2 (km s^{-1})	Vp/Vs
1	0–3	1.1–2.5	1.1–2.7	1.75–2.20
2	2–8	2.0–3.5	2.0–3.8	1.70–2.00
3	2–10	2.8–4.0	3.0–4.0	1.65–2.00
4	2–12	3.4–4.5	3.4–4.5	1.65–1.90
5	5–20	4.0–4.7	4.2–4.7	1.70–1.85
6	5–25	4.2–5.0	4.4–5.0	1.70–1.85

Parameter space bound used in the receiver function inversion. H, a layer thickness (km); Vs_1, the *S*-wave velocity at the top of a layer (km s^{-1}); Vs_2, the bottom of a layer (km s^{-1}); *Vp/Vs*, the velocity ratio in a layer.

made by Radha Krishna *et al.* (2002) through modelling of gravity field measurements. An Airy crustal thickness (T_c) of 17 ± 2 km for the Laccadive is suggested by Chaubey *et al.* (2008). Admittance analysis of satellite-derived gravity data and bathymetric data shows the low effective elastic thickness ($T_e = 2$ km) and the depth of compensation is 18–20 km in the Laccadive region (Tiwari *et al.* 2007). As crustal thickness obtained from isostatic studies is always less than actual crustal thickness (Detrick & Watts 1979; McAdoo & Sandwell 1989), our observation of present day Moho depth of 24 km is in agreement with these studies.

White *et al.* (1992), based on the seismic and rare earth element data, classified oceanic crust as: Normal oceanic crust (thickness 6–9 km), anomalous oceanic crust (slow spreading ridges and fracture zones: 2–6 km), plume affected oceanic crust (9–12 km) and crust generated directly above a mantle plume (19–22 km). Recent geophysical data shows thick layer with high seismic wave velocity ($Vp = 7.4$–7.8 km s^{-1}) at the base of the crust beneath several other islands like Marquesas (Caress *et al.* 1995), Hawaiian island (Watts *et al.* 1985), Réunion (Charvis *et al.* 1999) and the Cook, Society and Line islands (Leahy & Park 2005) and all are linked to hotspot tracks.

To the north of the CLR, between 15° and 18°N, Naini & Talwani (1982) identified isolated structure, named as Laxmi ridge, with very unusual crustal structure—the Moho at depth greater than 21 km and high velocity layer ($Vp > 7.2$ km s^{-1}) between 13 and 21 km. We compared the velocity (*Vp)* structure of the Laccadive ridge with the Laxmi ridge and the Reunion Island (Fig. 7). Both the ridges, Laxmi and Laccadive show similarity in terms of their

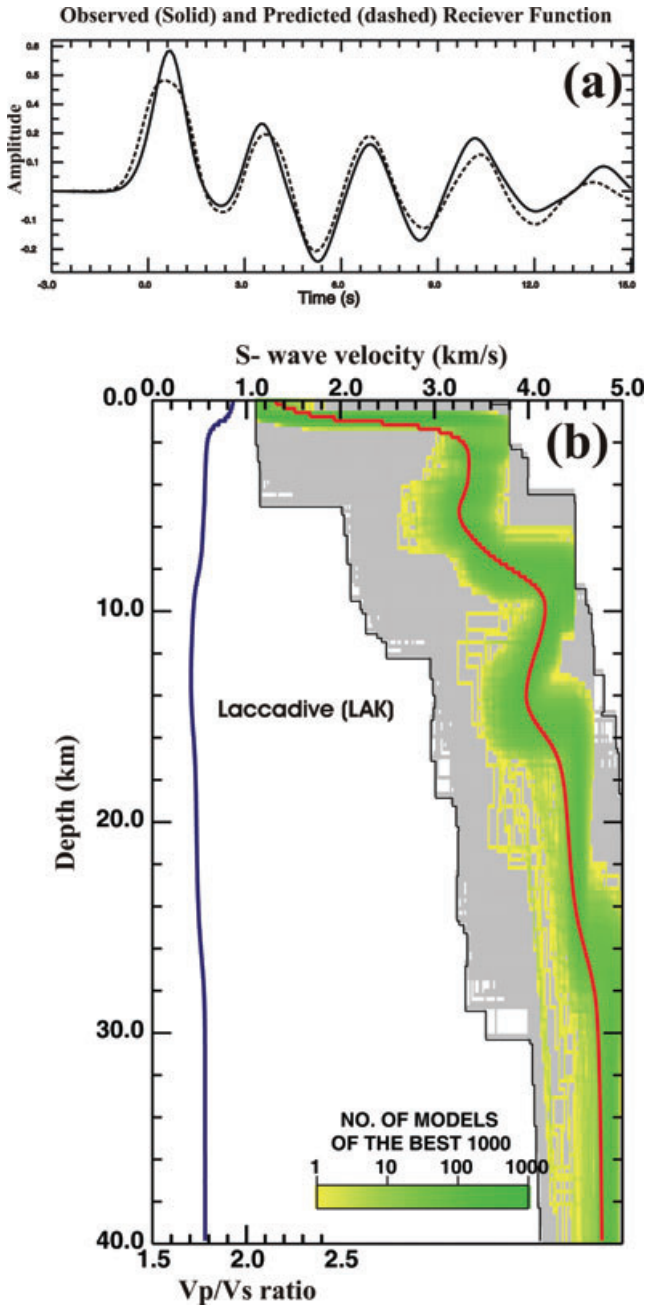

Figure 5. Inversion results for LAK station. (a) Observed (solid line) versus calculated (dashed line) stacked receiver function gathers for the minimum misfit velocity model, as shown by the red line in (b). (b) Seismic *S*-wave velocity models resulting from non-linear inversion. The full range of the 20 100 models searched in the inversion is shown by the outline of the light grey shading. The shaded (green) regions indicate the density of the 1000 best models, the colour being logarithmically proportional to the number of models, as shown by the scale bar. The solid red line represents the mean of the best 1000 models. The *Vp/Vs* ratio for the best model is shown on the left side (blue line) of the models.

unusual thickness and underplating. Considering that the Reunion Island is formed over a young ocean floor, magmatic underplating is a common factor in all the three, namely Reunion, Laccadive and Laxmi ridge. This leads us to hypothesize that all the three are on the trace of the Reunion hotspot and are altered by the same source.

In the NE Indian Ocean, thick crust with underplated lower crust was reported beneath the isostatic compensated central part of Ninety-East ridge (Grevemeyer *et al.* 2001) and is intrepretated as formed due to interaction of Kergulean hotspot with Wharton fossil spreading ridge axis (Tiwari *et al.* 2003). Our inference of a thick crust with underplated lower crust, which is locally isostatically compensated, can also be alternately interpreted as consequence of the interaction of hotspot with the spreading ridge axis. However, trace element compositions of basalts from Site 715 (Fig. 1) suggest that the Reunion hotspot was not located at a spreading ridge because there is little evidence for large-scale mixing with magmas of a mid-ocean ridge origin (Fisk *et al.* 1989). Also, Palegeographic reconstruction of the western Indian Ocean and volcanic record of the Reunion hotspot indicate that during 56–57 Ma, the Reunion hotspot was building the volcanic island drilled into at Site 715 (Fig. 1) and was never centred directly below a spreading centre (Duncan 1990).

6 CONCLUSION

The inferences from our study and its correlation with other investigations allow us to speculate the following possible geodynamic processes that operated on the Laccadive island.

Rapidly northward drifting Indian plate, from Cretaceous till early Oligocene at about 8–10 cm yr^{-1} (Duncan 1981), over the Reunion mantle plume created thermal erosion of the lithosphere and created a reservoir of primary melt at the lithosphere–asthenosphere boundary. Magma was rapidly transported in a short time (Courtillot *et al.* 1986) from the reservoir to the surface followed by cooling and fractionation at the crust–mantle boundary. Since the Moho represents a density and/or a rheological boundary that inhibits the ascent of the partial melt, mafic cumulate formed during fractionation of the picritic mantle melt flowed laterally at this boundary. This underplated material exhibits as the high velocity layer in the depth 16–24 km and forms the base of present day thickened crust beneath the Laccadive Island.

We also find similarity between the crustal structure of the Laccadive and the Laxmi ridge in terms of unusual crustal thickness and presence of underplated layer. In addition, we observe that these ridges and the Reunion Island have commonality through presence of high velocity layer. We speculate that such a feature has common genetic link with the hotspot and the path from the Laxmi ridge to the Reunion Island form the trace of the Reunion hotspot. This study along with other global investigations suggests that the crustal underplating is characteristic of the hotspot linked oceanic islands. The deep structure of the Laccadive Island is still poorly known and obtained velocity model combining with more data from an integrated study would certainly provide with a better understanding of the formation of the Laccadive Island and would contribute to understand the geodynamics in NW Indian ocean.

ACKNOWLEDGMENTS

The experiment was supported by a research grant from Deep Continental Studies Programmes, Department of Science and Technology, New Delhi. We thank Prof. M. Sambridge for providing inversion software used in this study and Dr. V.M. Tiwari for useful discussions. The figures are made by using GMT (Wessel & Smith 1998). Dr. Ingo Grevemeyer, the Editor and one anonymous reviewer provided constructive comments and suggestions, which helped us to improve the manuscript.

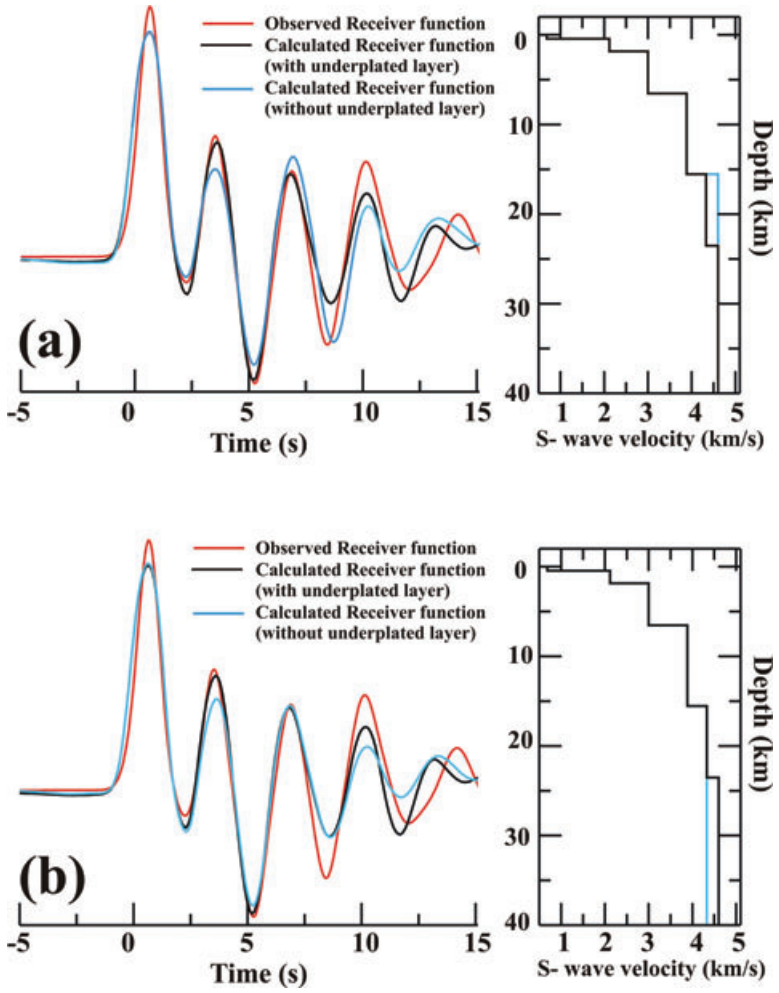

Figure 6 (a) and (b) Results of synthetic tests with varying velocity in the depth 16–24 km (right panel) and corresponding calculated receiver functions (left panel). Red colour shows the observed receiver function. Black and blue colour shows velocity models and corresponding calculated receiver functions with and without high velocity lower crustal layer, respectively.

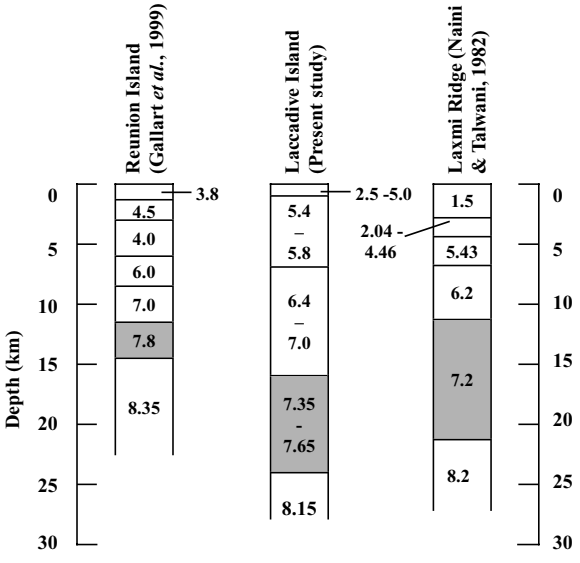

Figure 7. Average *P*-wave velocity for the crust from the Reunion Island (Gallart *et al.* 1999), Laxmi Ridge (Naini & Talwani 1982) and Laccadive (this study). Presence of crustal underplating (marked in grey) is common to three regions and possibly the trace of Reunion hotspot.

REFERENCES

Caress, D.W., McNutt, M.K., Detrick, R.S. & Mutter, J.C., 1995. Seismic imaging of hotspot-related crustal underplating beneath the Marquesas Islands, *Nature,* **373,** 600–603.

Charvis, Ph. *et al*., 1999. Spatial distribution of hotspot material added to the lithosphere under La Réunion, from wide-angle seismic data, *J. geophy. Res.,* **104,** 2875–2893.

Chaubey, A.K., Srinivas, K., Ashalatha, B. & Rao, D.G., 2008. Isostatic response of the Laccadive Ridge from admittance analysis of gravity and bathymetry data, *J. Geodyn.,* **46,** 10–20.

Christensen, N.I. & Salisbury, M.H., 1975. Structure and constitution of the lower oceanic crust, *Rev. Geophys. Space Phys.,* **13,** 57–86.

Courtillot, V., Besse, J., Vandamme, D., Montigny, R., Jaeger, J.J. & Cappetta, H., 1986. Deccan flood basalts at the Cretaceous/Tertiary boundary? *Earth planet. Sci. Lett.,* **80,** 361–374.

Detrick, R.S. & Wattts, A.B., 1979. An analysis of isostasy in the world's ocean, 3, Aseismic Ridges, *J. geophy. Res.,* **84,** 3637–3653.

Duncan, R.A., 1981. Hot spots in the southern oceans–an absolute frame of reference for motion of the Gondwana continents, *Tectonophysics,* **74,** 29–42.

Duncan, R.A., 1990. The volcanic record of the Reunion hotspot, in *Proceedings of the Ocean Drilling Program, Scientific Results,* Vol. 115, pp. 3–10, eds Duncan, R.A., Backman, J., Peterson, L.C. *et al*., Ocean Drilling Program, College Station, TX.

Farnetani, C.G., Mirachards, M.A. & Ghiroso, M.S., 1996. Petrological models of magmaevolution and deep crustal structure beneath hotspots and flood basalt provinces, *Earth planet. Sci. Lett.,* **143,** 81–94.

Fisk, M.R., Duncan, R.A., Baxter, A.N., Greenough, J.D., Hargraves, R.B., Tatsumi, Y. & Shipboard Scientific Party, 1989. Reunion hotspot magma chemistry over the past 65 m.y.: results from Leg 115 of the Ocean Drilling Program, *Geology,* **17,** 934–937.

Francis, T.J.G. & Shor, G.G., 1966. Seismic refraction measurements in the Northwest Indian Ocean, *J. geophy. Res.,* **71,** 427–449.

Gallart, J., Driad, L., Charvis, P., Sapin, M., Hirn, A., Diaz, J., Voogd, B. & Sachpazi, M., 1999. Perturbation to the lithosphere along the hotspot track of La Reunion from an offshore-onshore seismic transect, *J. geophy. Res.,* **104,** 2895–2908.

Grevemeyer, I., Flueh, E.R., Reichert, C., Bialas, J., Klaschen, D. & Kopp, C., 2001. Crustal architecture and deep structure of the Ninetyeast ridge hotspot trail from active-source ocean bottom seismology, *Geophys. J. Int.,* **144,** 414–431.

Leahy, G.M. & Park, J., 2005. Hunting for oceanic island Moho, *Geophys. J. Int.,* **160,** 1020–1026.

Ligorria, J.P. & Ammon, C.J., 1999. Iterative deconvolution and receiver function estimation, *Bull. Seismol. Soc. Am.,* **89,** 1395–1400.

McAdoo, D.C. & Sandwell, D.T., 1989. On the source of cross-grain lineations in the central Pacific gravity field, *J. geophy. Res.,* **94,** 9341–9352.

Morgan, W.J., 1972. Deep mantle convection plumes and plate motions, *Am. Assoc. Petrol. Geol. Bull.,* **56,** 203–213.

Naini, B.R. & Talwani, M., 1982. Structural framework and the evolutionary history of the continental margin of western India, in *Studies in Continental Margin Geology,* Vol. 34, pp. 167–191, eds Wakins, J.S. & Drake, C.L., Am. Assoc. Pet. Geol. Mem. Tulsa, OK.

Pichon X.L., Houtz, R.E., Drake, C.L. & Nafe, J.E., 1965. Crustal structure of the Mid-Ocean Ridges, *J. geophy. Res.,* **70,** 319–339.

Radha Krishna, M., Verma, R.K. & Purustham, A.K., 2002. Lithospheric structure below the eastern Arabian Sea and adjoining West Coast of India based on integrated analysis of gravity and seismic data, *Mar. Geophys. Res.*, **23,** 25–42.

Sambridge, M., 1999. Geophysical inversion with a neighbourhood Algorithm-I searching a parameter space, *Geophys. J. Int.,* **138,** 479–494.

Sambridge, M., 2001. Finding acceptable models in nonlinear inverse problems using a neighbourhood algorithm, *Inverse Probl.*, **17,** 387–403.

Schlich, R., 1982. The Indian Ocean: aseismic ridges, spreading centers, and oceanic basins, in *The Ocean basins and margins,* Vol. 6, pp. 51–148, eds Nairn, A.E.M. & Stehli, F.G., Plenum Press, New York.

Tiwari, V.M., Diament, M. & Singh, S.C., 2003. Analysis of satellite gravity and bathymetery data over Ninety-East Ridge: variation in the composition mechanism and implication for emplacement process, *J. geophy. Res.,* **108,** doi:10.1029/2000JB000047.

Tiwari, V.M., Greveemeyer, I., Singh, B. & Morgan, J.P., 2007. Variation of effective elastic thickness and melt production along the Deccan-Reunion hotspot track, *Earth planet. Sci. Lett.,* **264,** 9–21.

Watts, A.B., ten Brink, U.S., Buhl, P. & Brocher, T.M., 1985. A multichannel seismic study of lithosphere flexure across the Hawaiian-Emperor seamount chain, *Nature,* **315,** 105–111.

Wessel, P. & Smith, W., 1998. New, improved version of the generic mapping tools released. *EOS Trans. Am. geophy. Un.,* **79,** 579.

White, R. & McKenzie, D., 1989. Magmatism at rift zones: the generation of volcanic continental margins and flood basalts, *J. geophys. Res.,* **94,** 7685–7729.

White, R., McKenzie, D. & O'Nions, R.K., 1992. Oceanic crustal thickness from seismic measurements and rare earth element inversion, *J. geophys. Res.,* **97,** 19 683–19 715.

Whitmarsh, R.B. *et al*., 1974. *Initial Reports of the Deep-Sea Drilling Project,* Vol. 23, pp. 35–115, U.S. Government Printing Office, Washington, D.C.

Wilson, J.T., 1963. A resume of the geology of islands in the main ocean basin, in *Atlantic and Indian oceans, Sci. Rep.,* Vol. **4**(1), pp. 50–75, University of Toronto, Toronto, Ont., Canada.